ResearchGate

See discussions, stats, and author profiles for this publication at: https://www.researchgate.net/publication/229897541

Crazing in Two and Three Dimensions. 2. Three-Dimensional Crazing

ARTICLE *in* MACROMOLECULES · JULY 1999

Impact Factor: 5.8 · DOI: 10.1021/ma9810159

CITATIONS
10

READS
28

2 AUTHORS, INCLUDING:

Glenn H Fredrickson
University of California, Santa Barbara
434 PUBLICATIONS **28,369** CITATIONS

SEE PROFILE

Available from: Glenn H Fredrickson
Retrieved on: 26 January 2016

Crazing in Two and Three Dimensions. 1. Two-Dimensional Crazing

T. N. Krupenkin*

Bell Labs, Lucent Technologies, 600 Mountain Avenue, Murray Hill, New Jersey 07974

G. H. Fredrickson

Materials Research Laboratory, University of California, Santa Barbara, California 93106

Received June 29, 1998; Revised Manuscript Received April 1, 1999

ABSTRACT: A simple model is proposed to describe crazing in a very thin polymer film. It is argued that if the thickness of the film is below a certain critical value, the craze microstructure becomes similar to the deformation zone (two-dimensional neck) with the superimposed fibril structure. Deformation zone profile, characteristic fibril size, draw ratio, and critical film thickness are calculated as functions of material parameters and imposed strain rate. The results obtained are in good agreement with experimental values. The predictions of the model can also be used to verify the model of crazing in thick films and bulk polymers, which is described in Part 2 of the present series.

1. Introduction

Crazing in polymeric materials constitutes a problem of both fundamental and technological significance. Crazes greatly reduce the energy necessary for crack propagation in polymers and thus prevent them from exhibiting their ultimate toughness. The phenomenon of crazing was a subject of numerous studies over the last two decades, and a wealth of information, especially of experimental nature, can be found in the literature.[1−25] A number of excellent review papers[26−32] are also available.

Despite considerable advances in our understanding of crazing, we still lack its reliable theoretical description in many important situations, including crazing in thin polymer films and multilayered structures.[17,18,26] Detailed understanding of crazing necessarily includes description of several interrelated processes such as craze initiation, craze tip advance, craze thickening, and craze breakdown. Among those processes, craze thickening is especially important since it is responsible for the bulk of the energy dissipation during crazing and thus directly influences polymer toughness. In the current work, we are concerned with the craze-thickening phenomenon. Although crazes can be found in a wide range of polymeric materials, including both glassy and semicrystalline polymers, we restrict our attention to crazes in polymer glasses. We further limit the scope of the problem by considering only the case where no chain pullout or disentanglement takes place. This effectively means that we limit our attention to the high-molecular-weight materials at temperatures well below their glass-transition temperature, where no chain pullout is possible. We start with the description of crazing in very thin polymer films and later, in the second part of this series, address crazing in thicker films and bulk polymeric materials.

The microstructure of a craze in a polymer film strongly depends on the film thickness; see Figure 1. If the thickness of the film is above some critical value (which is usually on the order of 10^2 nm) craze structure can be described as a network of fine fibrils with the characteristic diameter on the order of 10^1 nm.[26,27] However, if the thickness of the film is below the critical thickness, craze microstructure essentially represents a two-dimensional (2D) neck, or deformation zone (DZ), with periodic variations of the neck thickness that somewhat resemble a superimposed fibril structure with occasional holes between fibrils.[17,18] Below, we will call such crazes two-dimensional (2D) crazes to distinguish them from the regular three-dimensional (3D) crazes encountered in thick films and bulk polymers. It is important to notice that although 2D crazes and deformation zones are similar structures, they are not identical. Deformation zones can exist in both thick and thin films. They are usually formed by ductile polymers that under normal conditions exhibit shear deformation, rather than crazing. On the other hand, 2D crazes can exist only in very thin films. They are formed by polymers that under normal conditions develop regular 3D crazes. Fibril-like variations in the neck thickness are exhibited by 2D crazes but not by deformation zones.

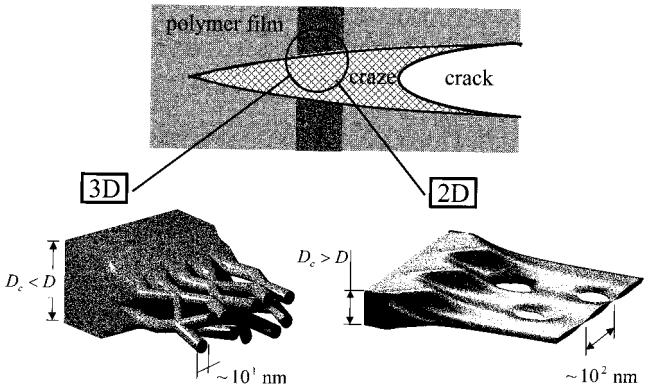

Figure 1. Dependence of craze microstructure on film thickness. If thickness D of the film is above some critical value D_c (which is usually on the order of 10^2 nm) craze structure can be described as a network of fine fibrils with a characteristic diameter on the order of 10^1 nm (3D craze). However, if the thickness of the film is below the critical thickness, craze microstructure essentially represents a 2D neck with the periodic variations of the neck thickness that somewhat resemble a superimposed fibril structure with occasional holes between fibrils (2D craze).

In a 2D craze, the average size of craze fibrils is considerably larger than the corresponding size (diameter) of the regular craze fibrils in thick films. For instance, in a 100 nm film of PS, the fibril characteristic

10.1021/ma981014g CCC: $18.00 © xxxx American Chemical Society
Published on Web 00/00/0000 PAGE EST: 6.7

size is 50−150 nm, while in thick PS films and bulk PS crazes, it is 10−12 nm.[17,18,26] The craze-thickening stress σ_c in thin films is close to that in thick films.[17,18] However, there is a considerable difference in the natural draw ratio in 2D and 3D crazes. Natural draw ratio λ is defined as a ratio of the values of the cross-sectional area at the front and at the rear part of the neck or DZ. It is sometimes compared with the so-called maximum microscopically allowed entanglement strand elongation λ_{st}.[18,26,27] The latter is a microscopic quantity defined as the maximum possible elongation of a polymer chain piece with an end-to-end distance equal to the average distance between entanglements. The natural draw ratio in 2D crazes is approximately equal to $\lambda^{(2D)} \approx 0.6\lambda_{st}$,[18,33−36] while in 3D crazes, it is typically higher and is equal to $\lambda^{(3D)} \approx 0.9\lambda_{st}$.[26−28,31] At this point, we would like to note that the above relationships are satisfied everywhere within the craze zone except for the midrib, where λ often exceeds λ_{st}. Since the midrib zone is formed at the craze tip during its advance to the virgin polymer, it will not be considered in the present work, and we will confine our attention to the main craze zone, where $\lambda \leq \lambda_{st}$.

Our first goal is to construct a model capable of describing the process of thickening of 2D crazes. In particular we are interested in calculating DZ profiles, draw ratio λ, fibril size, and the maximum film thickness at which a steady-state growth of 2D crazes is still possible. The paper is organized in the following manner. In section 2, we discuss a constitutive relationship that is used in the model to describe the stress−strain behavior of a polymer glass. In the next section, we address necking in ductile polymers. Comparison of the draw ratio in 2D and 3D crazes is discussed in section 4. Two-dimensional crazes are described in section 5, and the origin of the fibril structure in 2D crazes is investigated in section 6. Discussion of results obtained and conclusions are given in section 7.

2. Constitutive Relationship

As the first step toward constructing our model, we need to adopt some constitutive relationship connecting stress, strain, and strain rate. Stress−strain behavior of a polymer glass during elongation can be described by the following equation:[37,38]

$$\sigma(\lambda,\dot{\lambda}) = Y(\dot{\lambda}) + G_p(\lambda^2 - 1/\lambda) \tag{1}$$

where σ is the value of tensile stress in the direction of elongation, λ is elongation (dimensionless extension ratio), G_p is the strain hardening modulus, and $Y(\dot{\lambda})$ is a function of elongation rate $\dot{\lambda}$ and temperature. Such a phenomenological relationship that approximates the total stress as a sum of contributions due to strain and strain rate has been shown by Haward[37,38] to describe reasonably well plastic deformation and necking in a number of glassy and semicrystalline polymers. The main problem with the second term in eq 1, which defines the dependence of stress on strain, is that it describes neither initial effects like strain softening nor large-strain situations, where λ approaches λ_{st}. At the first glance, this might appear to be a potentially serious problem, since both strain softening and strain hardening are likely to take place at some point during crazing. However, as we will see later, in the crazing polymer, the main contribution to stress σ comes not from the strain itself but from the strain rate, i.e., from the term $Y(\dot{\lambda})$. Thus, the shortcomings of the $\sigma(\lambda)$ dependence will not substantially affect the model.

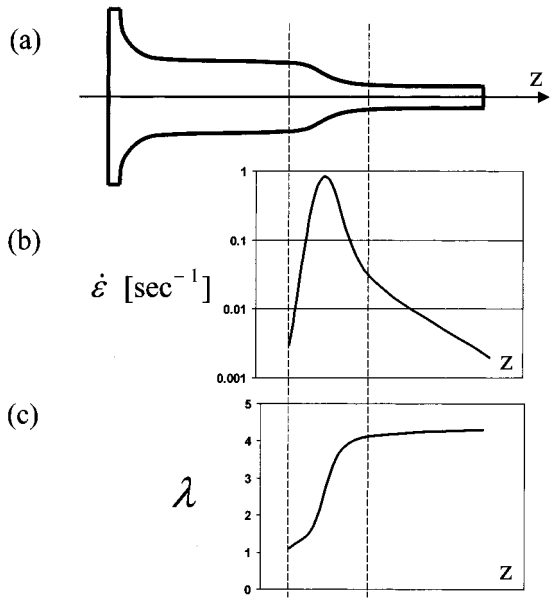

Figure 2. (a) Neck profile, (b) strain rate variation $\dot{\epsilon}(z)$, and (c) draw ratio profile $\lambda(z)$ for the 3×10^5 molecular weight polyethylene. Adapted from Coates and Ward.[40]

With respect to the form of the function $Y(\dot{\lambda})$ (or $Y(\dot{\epsilon})$, where $\epsilon = \ln \lambda$) one can find in the literature two different relationships. The first, based on the Eyring theory of viscosity, is[38]

$$Y(\dot{\epsilon}) = \frac{1}{B} \ln\left(\frac{\dot{\epsilon}}{A}\right) \tag{2}$$

where A and B are temperature-dependent constants that describe the material under consideration. The second is power law fluid[26,27]

$$Y(\dot{\epsilon}) = \sigma_{fc}\left(\frac{\dot{\epsilon}}{\dot{\epsilon}_f}\right)^{1/n} \tag{3}$$

where σ_{fc}, $\dot{\epsilon}_f$, and $n \gg 1$ are material parameters. The main problem with both of these relationships is that the limit $Y(\dot{\epsilon} \to 0)$ is not an equilibrium yield stress σ_{0y}, as it is known to be from experiment.[41] For our model that deals with necking and cold drawing phenomena, the main implication is that the neck (DZ) profiles will be inaccurately described at the region close to the very beginning of the neck, where $\dot{\epsilon} \to 0$; see Figure 2. In particular, instead of the smooth joint between the neck and the slab of the material, the neck and the slab will be joined with some finite angle. In the further discussion, we will use eq 2 for $Y(\dot{\epsilon})$. However, eq 3 should also give similar results, provided appropriate values are used for material parameters. It is important to notice that under normal testing conditions the ratio $Y(\dot{\epsilon})/G_p$ is quite high for the majority of crazing polymers. For instance, Haward estimates $Y(\dot{\epsilon})/G_p$ as 54 for PTBS, 32 for PS, and 7 for PMMA.[37] At the same time, very ductile polymers tend to have $Y(\dot{\epsilon})/G_p$ on the order of one.[37] As we will see, this fact has important consequences for the natural draw ratio in ductile and crazing polymers.

3. Necking in Ductile Polymers

Let us first consider a general case where both terms in eq 1 are on the same order and we cannot neglect

any of them. Our first goal is to formulate the conditions on the material parameters at which a stable neck propagation is possible. To this end, we want to calculate strain rate as a function of the draw ratio of the neck using eqs 1 and 2. We assume that the neck propagates with the constant velocity v_0 while the thread take-up (drawing) velocity is v_{ext}, which is defined by the experimental setup. In the reference frame of the neck, the material is then entering the neck with velocity v_0 and is exiting the neck with velocity $v_m = v_0 + v_{ext}$. We assume that both the material flux Q and the total force F are conserved along the neck and neglect variations of stress and velocity along the neck cross section. We then have

$$v_0 S_0 = v(z)S(z) = Q = \text{const} \tag{4}$$

$$\sigma_{0y} S_0 = \sigma(z)S(z) = F = \text{const} \tag{5}$$

where S_0 is initial cross-sectional area, $S(z)$ is cross-sectional area at point z along the neck, σ_{0y} is the equilibrium yield stress (yield stress at $\dot{\epsilon} \to 0$), and $\sigma(z)$ is the stress at point z. We define the draw ratio λ at point z along the neck as

$$\lambda(z) = \frac{S_0}{S(z)} \geq 1 \tag{6}$$

We then have

$$v(z) = \lambda(z)v_0$$

$$\sigma(z) = \lambda(z)\sigma_{0y} \tag{7}$$

Strain is defined as

$$\epsilon = \ln \lambda \tag{8}$$

and strain rate as

$$\dot{\epsilon} = \frac{\dot{\lambda}}{\lambda} = \frac{dv}{dz} = v_0 \frac{d\lambda}{dz} \tag{9}$$

We denote the draw ratio at the end of the neck as λ_m, the maximum draw ratio. We then have

$$v_0 = \frac{v_{ext}}{\lambda_m - 1} \tag{10}$$

$$v_m = v_0 \lambda_m \tag{11}$$

We can now formulate the following system of equations

$$\sigma = \lambda\sigma_{0y}$$

$$\sigma = G_p\left(\lambda^2 - \frac{1}{\lambda}\right) + \frac{1}{B}\ln\left(\frac{\dot{\epsilon}}{A}\right) \tag{12}$$

The solution of this system with respect to $\dot{\epsilon}(\lambda)$ takes the form

$$\dot{\epsilon} = A \exp\{B\,[\sigma_{0y}\lambda - G_p(\lambda^2 - 1/\lambda)]\} \tag{13}$$

We should note here that since eq 1 is equally applicable to amorphous and semicrystalline polymers, eq 13 can also be applied to both groups of materials. One of the best materials that can be used to test eq 13 is polyethylene, since both its true stress−strain behavior and its necking behavior were studied to a great degree of detail. Thus, using the values of parameters A, B, G_p, and σ_{0y} evaluated from the data in the literature,[38,39] we can successfully reproduce the $\dot{\epsilon}(\lambda)$ curves obtained by Coates and Ward[40] for the cold drawing of polyethylene; see Figure 3. One can go further and use eq 9 and 13 to calculate the neck profile described by $\lambda(z)$ and $\dot{\epsilon}(z)$ dependencies that also turn out to be in agreement with experimental data reported in reference.[40] We will not describe these calculations here since they are not directly related to our present goal. A detailed analysis of the neck profiles can be found in a number of papers including the work of Coates and Ward,[40] Haward,[38] and Hutchinson and Neale.[44]

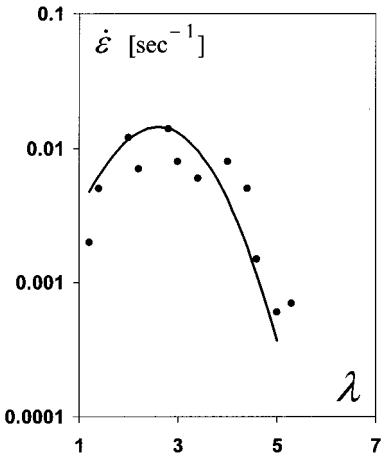

Figure 3. Variation of the strain rate with draw ratio in 3×10^5 molecular weight polyethylene. Experimental points are from Coates and Ward.[40] The solid line corresponds to eq 13. Parameters are chosen as $A = 6.19 \times 10^{-5}$ s^{-1}, $B = 0.217$ MPa^{-1}, $G_p = 3$ MPa, and $\sigma_{0y} = 16$ MPa.

We now explore conditions under which eq 13 describes a steady-state neck propagation. In order to describe a neck, the function $\dot{\epsilon}(\lambda)$ must have a maximum at $\lambda > 1$. Indeed, material enters and exits the neck with $\dot{\epsilon} \to 0$ (see Figure 2), and thus, if $\dot{\epsilon}(\lambda)$ is greater than zero, it must have a maximum at some $\lambda_1 > 1$. Using the equation

$$(d\dot{\epsilon}/d\lambda)_{\lambda=\lambda_1} = 0 \tag{14}$$

where $\lambda_1 > 1$, we obtain

$$\frac{\sigma_{0y}}{G_p} = 2\lambda_1 + \lambda_1^{-2} \tag{15}$$

We thus see that a steady-state neck propagation in the material with the strain hardening described by eq 1 is possible only if σ_{0y}/G_p ratio is greater than 3. The materials with $\sigma_{0y}/G_p < 3$ have too strong of a strain hardening effect to form a neck. From eq 15, we see that the materials that tend to craze and have $\sigma_{0y}/G_p \gg 1$ should also have $\lambda_1 \gg 1$ and thus $\lambda_m \gg 1$. Such values of λ well exceed the maximum microscopically allowed entanglement strand elongation λ_{st}.[26,27] Since in real materials λ_m cannot exceed λ_{st}, crazing polymers reach a stable neck (DZ) at $\lambda_m \to \lambda_{max}$, where $\lambda_{max} \leq \lambda_{st}$ is the maximum microscopically allowed draw ratio.

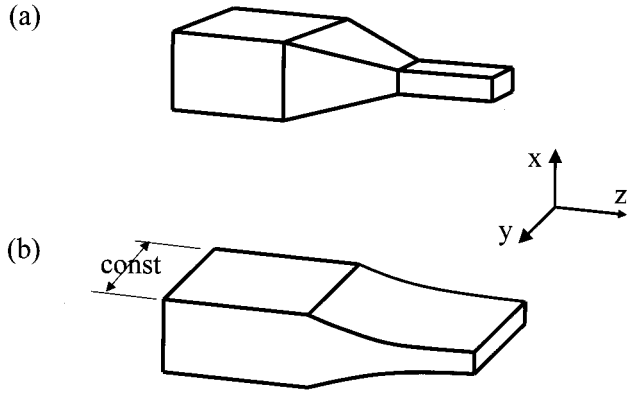

Figure 4. (a) In a regular neck, slab shrinking in both x and y directions while being elongated in z direction. (b) In a 2D neck, slab shrinking in x direction while being elongated in z direction.

4. Draw Ratio in 2D and 3D Necks

Let us consider the case where $\sigma_{0y}/G_p \gg 1$ and the neck is stabilized at $\lambda \to \lambda_{max}$. Our goal is to find the difference between λ_{max} in a regular neck (3D neck) and a DZ (2D neck). The only geometrical difference between a 2- and a 3D neck is that in a 3D neck all three dimensions are allowed to change, while in a 2D neck one dimension transverse to the neck is kept constant; see Figure 4. Let us for simplicity describe a polymer chain as a random walk on a cubic lattice with the lattice constant a. We consider a piece of the chain with N monomers and an end-to-end distance equal to the distance l_{ent} between entanglements. We define maximum strand extension λ_{st} as the ratio of the contour length l_{cont} of this chain piece to its end-to-end distance

$$\lambda_{st} = \frac{l_{cont}}{l_{ent}} = \frac{Na}{a\sqrt{N}} = \sqrt{N} \tag{16}$$

When the chain is in a virgin piece of the polymer, it has (on average) an equal number of vectors (random walk steps) oriented along x, y, and z axes

$$N_{0x} \approx N_{0y} \approx N_{0z}$$
$$N = N_{0x} + N_{0y} + N_{0z} \tag{17}$$

Suppose now that this piece of the polymer is moved through the 3D neck and is extended to its maximum draw ratio $\lambda_{max}^{(3D)}$. Then, all the vectors originally oriented along the x and y axes are now reoriented along the z axis, as shown in Figure 5a. Then, the chain is extended to its full length, and thus, the draw ratio $\lambda_{max}^{(3D)}$ defined as the ratio of the chain new end-to-end distance to the original distance takes the form

$$\lambda_{max}^{(3D)} = \frac{N_{0x} + N_{0y} + N_{0z}}{\sqrt{N}} = \lambda_{st} \tag{18}$$

However, if that same piece of the polymer was moved through a 2D neck, then vectors along y axis were not reoriented, since the neck dimension in this direction must be preserved; see Figure 5b. Thus,

$$\lambda_{max}^{(2D)} = \frac{N_{0x} + N_{0z}}{\sqrt{N}} = \frac{2}{3}\lambda_{st} \tag{19}$$

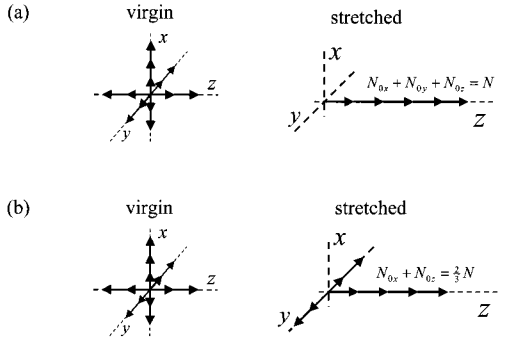

Figure 5. (a) Chain contraction in both x and y directions in a 3D neck. (All of the vectors can be stretched along the z axis). (b) Vectors along y axis unable be reoriented in a 2D neck. Thus the chain can be stretched to only $^2/_3$ of its length.

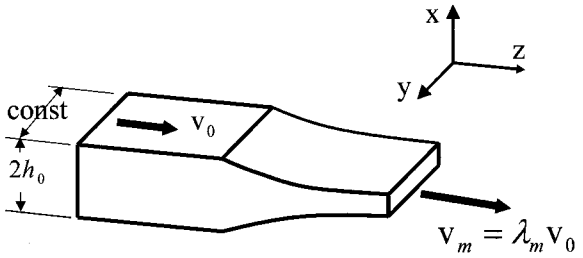

Figure 6. Material entering a 2D neck with constant velocity v_0 and exiting with velocity $v_m = \lambda_m v_0$. Initial thickness of the slab is $2h_0$. Neck dimension in y direction is preserved.

Thus, the natural draw ratio in a DZ is $\lambda_{max}^{(2D)} = (^2/_3)\lambda_{st}$, and in a regular neck, it is $\lambda_{max}^{(3D)} = \lambda_{st}$. The experimental data give $\lambda_{max}^{(2D)} \approx 0.6\lambda_{st}$ for DZ and $\lambda_{max}^{(3D)} \approx 0.9\lambda_{st}$ for 3D micronecks that give rise to individual craze fibrils.[18,26−28,31,33−36] As we can see, the agreement is reasonable.

5. Necking in Crazing Polymers

Let us now consider necking in polymers with $\sigma_{0y}/G_p \gg 1$. In this case, $Y(\dot{\epsilon})$ is a dominant term in eq 1. Thus, at the stresses above the yield stress, the polymer essentially behaves as a nonlinear viscous fluid. We now restrict our calculations to the case of a constant strain rate. In this case, we can describe a polymer as a simple Newtonian viscous fluid with some effective viscosity that corresponds to the chosen characteristic strain rate. The obvious advantage of a Newtonian fluid is its mathematical simplicity. The price we pay for this is linearized strain rate dependence of the resulting equations. Since a viscous fluid has no strain-hardening property, we have to impose an additional constraint that draw ratio λ of any element of the fluid cannot exceed its microscopically defined λ_{max}. Although ductile polymers can easily form macroscopically large necks, crazing polymers are known to form only very small necks with the characteristic size (diameter) of 10^1−10^2 nm for the micronecks that give rise to individual craze fibrils. For such small necks, one cannot neglect surface tension as was done in the consideration of necking in ductile polymers.

Let us now consider a 2D neck shown in Figure 6. Since we assume Newtonian fluid, we have

$$\sigma_{ii} = -p + 2\eta\frac{\partial v_i}{\partial i} \tag{20}$$

where σ_{ii} is the diagonal component of the stress tensor,

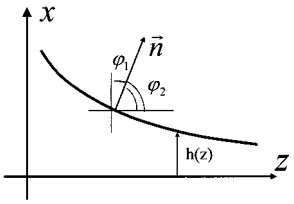

Figure 7. Laplace−Young boundary condition on the surface of the neck. See details in the text.

p is pressure, η is viscosity, v_i is a velocity component, and $i = x$, y, and z. Since we consider a 2D neck, we assume strip biaxial extension

$$\frac{\partial v_x}{\partial x} = -\frac{\partial v_z}{\partial z}$$

$$\frac{\partial v_y}{\partial y} = 0 \qquad (21)$$

We also assume conservation of total force F and flux Q along the neck and neglect variations of stress and velocity along the neck cross section

$$v_0 S_0 = v_z(z)S(z) = Q = \text{const}$$

$$\sigma_{0y} S_0 = \sigma_{zz}(z)S(z) = F = \text{const} \qquad (22)$$

where S_0 is initial cross-sectional area, $S(z)$ is cross-sectional area at point z along the neck, σ_{0y} is equilibrium yield stress, and $\sigma_{zz}(z)$ is the stress at point z. We define the draw ratio λ at point z along the neck as

$$\lambda(z) = S_0/S(z) = h_0/h(z) \qquad (23)$$

where $h(z)$ is one-half of the neck thickness at point z along the neck. We now adopt a Laplace−Young boundary condition at the free surface

$$f_n = \frac{\Gamma}{r(z)} \qquad (24)$$

where f_n is the normal component of the force acting on the surface of the fluid, $r(z)$ is the radius of the surface curvature at point z, and Γ is surface tension; see Figure 7. This boundary condition can be expressed as

$$\sigma_{xx}\cos^2\varphi_1 + \sigma_{zz}\cos^2\varphi_2 = \Gamma/r(z) \qquad (25)$$

where φ_1 and φ_2 are the angles between the vector $\vec{n}$ normal to the surface and the x and z axes, respectively; see Figure 7. The local curvature $r(z)$ is defined as

$$\frac{1}{r(z)} = \frac{\mathrm{d}^2h(z)}{\mathrm{d}z^2}\left\{1 + \left[\frac{\mathrm{d}h(z)}{\mathrm{d}z}\right]^2\right\}^{-3/2} \qquad (26)$$

Combining eq 20 through 26, we can obtain the following equation for the neck profile $h(z)$

$$\sigma_{0y}\frac{h_0}{h(z)} + 4\eta\frac{v_0}{h_0}\left[\frac{h_0}{h(z)}\right]^2\frac{\mathrm{d}h}{\mathrm{d}z}\left[1 + \left(\frac{\mathrm{d}h}{\mathrm{d}z}\right)^2\right]^{-1} = \Gamma\frac{\mathrm{d}^2h}{\mathrm{d}z^2}\left[1 + \left(\frac{\mathrm{d}h}{\mathrm{d}z}\right)^2\right]^{-3/2} \qquad (27)$$

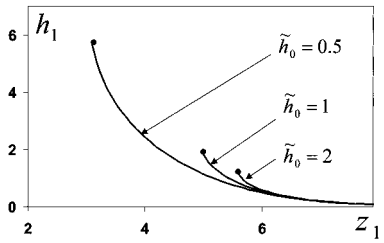

Figure 8. Numerical solution of eq 28. (Solution exists only for h_1 smaller than some maximum value.)

This equation can be rewritten in terms of dimensionless variables

$$\frac{1}{\tilde{h}_0}\frac{\mathrm{d}^2h_1}{\mathrm{d}z_1^2} - \frac{1}{h_1^2}\frac{\mathrm{d}h_1}{\mathrm{d}z_1}\left[1 + \left(\frac{\mathrm{d}h_1}{\mathrm{d}z_1}\right)^2\right]^{1/2} - \frac{1}{h_1}\left[1 + \left(\frac{\mathrm{d}h_1}{\mathrm{d}z_1}\right)^2\right]^{3/2} = 0 \qquad (28)$$

where

$$\tilde{h}_0 = \frac{h_0}{h^*} \quad \tilde{v}_0 = \frac{4\eta v_0}{\Gamma} \quad h^* = \frac{\Gamma}{\sigma_{0y}} \quad z_1 = \frac{z}{\tilde{v}_0 h^*} \quad h_1 = \frac{h}{\tilde{v}_0 h^*}$$

Let us now consider the case $\tilde{h}_0 \gg h_1^2$ which translates into

$$\eta v_0 \gg \frac{h}{4h_0}\sqrt{\Gamma h_0 \sigma_{0y}} \qquad (29)$$

As we will see later, this restriction is satisfied at the typical testing conditions. In this case, we can neglect the first term in eq 28. The resulting equation can be solved exactly and we obtain

$$z_1 + c = {}^1/_4[-2\sqrt{1 - 4h_1^2} + 2\,\mathrm{arctanh}\sqrt{1 - 4h_1^2} - \ln(4h_1^2)] \qquad (30)$$

where c is an integration constant defining the origin of the reference frame. For the case where $h_1^2 \ll 1$, eq 30 can be reduced to the well-known equation of a liquid jet

$$h = h_0 \exp(-z_1) \qquad (31)$$

From eq 30, we can see that a solution exists only if $h_1 < {}^1/_2$, which translates into the condition

$$h < 2\eta v_0/\sigma_{0y} \qquad (32)$$

This, in turn, means that the maximum thickness of the film that still can support a steady-state 2D neck propagation is

$$2\,h_{0\max} = 4\eta v_0/\sigma_{0y} \qquad (33)$$

For the case where v_0 is too small to satisfy eq 29, numerical solutions of eq 28 can be shown to have a similar property of having a maximum h_1 at which the solution still exists; see Figure 8.

6. Fibril Structure in a 2D Craze

Let us now consider the origin of the fibril structure that is superimposed on the 2D neck. The approach we use to analyze this problem is based on Suffman−Taylor

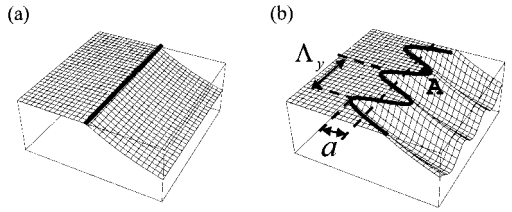

Figure 9. (a) Unperturbed neck propagation. The neck front is shown as a thick line. (b) Neck edge perturbed by a small perturbation described by eq 35. See details in the text.

(meniscus) instability mechanism.[42,43] This approach was successfully used by a number of authors including Fields and Ashby,[42] Argon and Salama,[43] and Donald and Kramer[19] to describe the development of fingerlike instabilities during craze/crack propagation in polymers and viscous fluids. We assume that the neck is propagating with the constant velocity v_0. We want to check whether the front of the neck, shown as a thick line on Figure 9a, is stable with respect to small fluctuations of its form. For the sake of mathematical simplicity, we assume that condition $h_1^2 \ll 1$ is satisfied. However, the following calculations can easily be modified to include the case of the general solution of eq 28. We thus use eq 31 to describe the neck profile

$$h(z) = h_0 \exp(-z/z_0) \tag{34}$$

where $z_0 = 4\eta v_0/\sigma_{0y}$. We assume that the edge of the neck, which is normally a straight line along the y axis, is perturbed by a small perturbation of the form

$$f(y) = a\cos\left(\frac{2\pi}{\Lambda_y}y\right) \tag{35}$$

where Λ_y is the perturbation wavelength and $a \ll z_0$ is the perturbation amplitude; see Figure 9b. The form of the neck is then described by the formula

$$h(y, z) = \min\{h_0, h[z + f(y)]\} \tag{36}$$

where $\min\{x, y\}$ denotes the minimum of x and y. Let us consider point A which is right at the edge of the neck as shown in Figure 9b. The change in the total stress at this point is defined as the sum of the additional stress gained by moving point A a distance a along the neck to the area of higher stresses

$$\Delta\sigma_{zz}^{(2)} = \sigma_{zz}(z = a) - \sigma_{zz}(z = 0) = \sigma_{zz}(z = a) - \sigma_{0y} \tag{37}$$

and the restricting stress due to surface tension

$$\Delta\sigma_{zz}^{(1)} = \frac{\Gamma}{R} \approx -\Gamma\left(\frac{\mathrm{d}^2 f(y)}{\mathrm{d}y^2}\right)_{y=0} = \frac{4\pi^2}{\Lambda_y^2}a\Gamma \tag{38}$$

The stress in the neck is defined by

$$\sigma_{zz}(z) = \sigma_{0y}S_0/S(z) \tag{39}$$

where S_0 is the cross-sectional area of the slab just in front of the neck and $S(z)$ is the cross-sectional area at point z along the neck. For the case where $z = a \ll z_0$, the function $S(z)$ can be approximated as (see Appendix)

$$S(z = a) \approx S_0\,(1 - a/z_0) \tag{40}$$

We then have

$$\sigma_{zz}(z = a) = \sigma_{0y}(1 + a/z_0) \tag{41}$$

and

$$\Delta\sigma_{zz}^{(2)} = \sigma_{0y}\,a/z_0 \tag{42}$$

For the excitation $f(y)$ to grow, we must have

$$\Delta\sigma_{zz}^{(2)} > \Delta\sigma_{zz}^{(1)} \tag{43}$$

This leads us to the condition on the wavelength of the instability that will grow with time

$$\Lambda_y > 2\pi\sqrt{z_0\Gamma/\sigma_{0y}} \tag{44}$$

This equation determines the smallest fibril size. It should be noted here that although eq 44 has a form similar to the known formula for the critical wavelength of the craze tip advance instability,[19] it describes quite a different physical situation. In the craze tip advance problem, meniscus instability develops in a viscometric flow of a strain-softened polymer between two rigid plates that represent the boundaries of the strain-softened layer. In this case, quantity z_0 is an adjustable parameter that represents a distance between these plates. In a 2D necking problem, meniscus instability develops during purely elongational flow, similar to the liquid jet flow. In this case, z_0 is not an adjustable parameter. For any given neck propagation velocity v_0, the value of z_0 is uniquely defined by the polymer effective viscosity η and its yield stress σ_{0y}; see eq 34.

Let us now make some numerical estimates. Crazing in thin PS films was studied by Kramer et al.[17,18] From these works, we can estimate $h_{0\max} \approx 50$ nm and $\sigma_{0y} \approx 20$ MPa. Substituting these data in eq 33, we can estimate the value of ηv_0 for that set of experiments as approximately 0.5 N/m. For eq 33 to be valid, the inequality of eq 29 has to be satisfied. Assuming that $\Gamma \approx 0.04$ N/m[27] and using the data above, we obtain $\eta v_0 \gg 0.07$ N/m and thus verify the validity of eq 33 for this set of experimental data. Finally, we can use eq 44 to calculate the minimum fibril size $\Lambda_y^{(\mathrm{cr})}$. After substitution, we obtain $\Lambda_y^{(\mathrm{cr})} \approx 88$ nm, which is in reasonable agreement with the experiment that puts the fibril size between 50 and 150 nm.[17,18]

7. Conclusions

In the present work, the process of craze thickening in a very thin polymer glass film is theoretically investigated. The microstructure of a craze in a thin film is described as a deformation zone (2D neck) with some superimposed fibril structure. It is demonstrated that such craze structure (2D craze) can exist only in films with the thickness below some critical value. In the model, this critical thickness is expressed as a simple function of strain rate, yield stress, and polymer effective viscosity. It is also demonstrated that due to simple geometrical constraints the natural draw ratio in a 2D craze can reach only $^2/_3$ of the draw ratio in a regular 3D craze. The origin of fibril structure in a 2D craze is investigated on the basis of Saffman−Taylor instability mechanism. The characteristic size of 2D craze fibrils is expressed as a function of the strain rate and material parameters.

Unfortunately, most of experimental data on crazing are related to crazing in thick films and bulk polymers. Thus, our ability to compare model predictions with experimental data is somewhat limited. However, in those cases where such comparison was possible (see sections 4 and 6) we obtained good quantitative agreement. The model of 2D crazing also serves as a first step towards development of the model of crazing in thick films and bulk polymers, which is introduced in Part 2 of the present series.

Acknowledgment. This work was supported by the MRL Program of the National Science Foundation under Award No. DMR96-32716. We thank Profs. Kramer, Donald, and Michler for their helpful comments and discussions.

Appendix

Neck Cross-Sectional Area. According to eq 34 and 36, the neck profile is defined as

$$h(y, z) = \min\{h_0, h_e\} \tag{A1}$$

where

$$h_e = h[z + f(y)] = h_0 \exp[-f(y)/z_0] \exp(-z/z_0) \tag{A2}$$

and $f(y)$ is defined by eq 35. Then cross-sectional area of the neck (per length Λ_y) is equal to

$$S(z) = h_0\Lambda_y - (y_2 - y_1)h_0 + \int_{y_1}^{y_2} h_e(y)\, dy \tag{A3}$$

where $-a \le z \le a$ and $y_{1,2}$ are solutions of equation $h_e(y,z) = h_0$. For the case where $-a \le z \le a$ these solutions take the form

$$y_{1,2} = \mp\Lambda y/(2\pi) \arccos(-z/a) \tag{A4}$$

Substituting eq A4 into eq A3 and assuming $z = a$, we obtain

$$S(a) = h_0\Lambda_y/(2\pi) \exp(-a/z_0) \int_{-\Lambda_y/2}^{\Lambda_y/2} \exp[-a/z_0 \times \cos(2\pi y/\Lambda_y)]\, dy \tag{A5}$$

If $a \ll z_0$, eq A5 can be approximated as

$$S(a) = h_0\Lambda_y(1 - a/z_0) = S_0(1 - a/z_0) \tag{A6}$$

References and Notes

(1) Hui, C. Y.; Kramer, E. J. *Poly. Eng. Sci.* **1995**, *35*, 419.
(2) Yang, C.-M. A.; Kunz, M. S.; Logan, J. A. *Macromol.* **1993**, *26*, 1767.
(3) Creton, C.; Kramer, E. J.; Hui, C. Y.; Brown, H. R. *Macromolecules* **1992**, *25*, 3075.
(4) Hui, C. Y.; Ruina, A.; Creton, C.; Kramer, E. J. *Macromolecules* **1992**, *25*, 3948.
(5) Brown, H. R. *Macromolecules* **1991**, *24*, 2752.
(6) Berger, L. L. *Macromolecules* **1990**, *23*, 2926.
(7) Miller, P.; Kramer, E. J. *J. Mater. Sci.* **1991**, *26*, 1459.
(8) Berger, L. L. *Macromolecules* **1989**, *22*, 3162.
(9) Brown, H. R.; Njoku, N. G. *J. Polym. Sci., Poly. Phys.* **1986**, *24*, 11.
(10) Michler, G. H. *Colloid Polym. Sci.* **1986**, *264*, 522.
(11) Michler, G. H. *Colloid Polym. Sci.* **1985**, *263*, 462.
(12) Kramer, E. J. *Polym. Eng. Sci.* **1984**, *24*, 761.
(13) Donald, A. M.; Kramer, E. J. *J. Mater. Sci.* **1982**, *17*, 1871.
(14) Donald, A. M.; Kramer, E. J. *J. Polym. Sci., Poly. Phys.* **1982**, *20*, 1129.
(15) Wang, W. C. V.; Kramer, E. J. *J. Mater. Sci.* **1982**, *17*, 2013.
(16) Donald, A. M.; Kramer, E. J. *J. Mater. Sci.* **1981**, *16*, 2977.
(17) Donald, A. M.; Chan, T.; Kramer, E. J. *J. Mater. Sci.* **1981**, *16*, 669.
(18) Chan, T.; Donald, A. M.; Kramer, E. J. *J. Mater. Sci.* **1981**, *16*, 676.
(19) Donald, A. M.; Kramer, E. J. *Philos. Mag.* **1981**, *43*, 857.
(20) Lauterwasser, B. D.; Kramer, E. J. *Philos. Mag.* **1979**, *39*, 469.
(21) Fraser, R. A. W.; Ward, I. M. *Polymer* **1978**, *19*, 220.
(22) Argon, A. S.; Salama, M. M. *Philos. Mag.* **1977**, *36*, 1217.
(23) Morgan, G. P.; Ward, I. M. *Polymer* **1977**, *18*, 87.
(24) Argon, A. S.; Salama, M. M. *Mater. Sci. Eng.* **1976**, *23*, 219.
(25) Brown, H. R.; Ward, I. M. *Polymer* **1973**, *14*, 469.
(26) Kramer, E. J. *Adv. Polym. Sci.* **1983**, *52/53*, 1.
(27) Kramer, E. J.; Berger, L. L. *Adv. Polym. Sci.* **1990**, *91/92*, 1.
(28) Döll, W.; Könczoll, L. *Adv. Polym. Sci.* **1990**, *91/92*, 137.
(29) Sauer, J. A.; Hara, M. *Adv. Polym. Sci.* **1990**, *91/92*, 70.
(30) Brown, H. R. *Mater. Sci. Rep.* **1987**, *2*, 315.
(31) Döll, W. *Adv. Polym. Sci.* **1983**, *52/53*, 105.
(32) Fredrich, K. *Adv. Polym. Sci.* **1983**, *52/53*, 225.
(33) Sanden, Van der; Meijer, H. E. H.; Lamstra, P. J. *Polymer* **1993**, *34*, 2148.
(34) Sanden, Van der; Meijer, H. E. H.; Tervoort, A. *Polymer* **1993**, *34*, 2961.
(35) Sanden, Van der; Meijer, H. E. H. *Polymer* **1993**, *34*, 5063.
(36) Sanden, Van der; Buijs, L. G. C.; Bie, F. O.; Meijer, H. E. H. *Polymer* **1994**, *35*, 2783.
(37) Haward, R. N. *Macromolecules* **1993**, *26*, 5860.
(38) Haward, R. N. *J. Polym. Sci., Polym. Phys.* **1995**, *33*, 1481.
(39) G'Sell, C.; Joans, J. J. *J. Mater. Sci.* **1981**, *16*, 1956.
(40) Coates, P. D.; Ward, I. M. *J. Mater. Sci.* **1980**, *15*, 2897.
(41) Zhon, Z.; Chudnovsky, A.; Bosnyak, C.; Sehanobish, K. *Polym. Eng. Sci.* **1995**, *35*, 304
(42) Fields, R. J.; Ashby, M. F. *Philos. Mag.* **1976**, *33*, 33.
(43) Argon, A. S.; Salama, M. M. *Philos. Mag.* **1977**, *36*, 1217.
(44) Hutchinson, J. W.; Neale, K. W. *J. Mech. Phys. Solids* **1983**, *31*, 405.

MA981014G